

MOL #101626

Correlation between activity and domain complementation in adenylyl cyclase demonstrated with a novel FRET sensor

Michael Ritt, Sivaraj Sivaramakrishnan

Department of Genetics, Cell Biology and Development, University of Minnesota, Minneapolis, MN 55455. MR, SS

MOL #101626

Domain complementation controls adenylyl cyclase activity

Corresponding Author:

Sivaraj Sivaramakrishnan

420 Washington Ave SE

4-130 MCB

Minneapolis, MN, 55455

612-301-1537

sivaraj@umn.edu

Number of text pages: 19

Number of tables: 0

Figures: 5

Supplemental figures: 3

References: 15

Number of words in-

Abstract: 120

Introduction: 470

Discussion: 666

Abbreviations: AC- adenylyl cyclase, dFSK- deoxyforskolin, ER/K helix- glutamine arginine/lysine helix FSK- forskolin, GTP γ S- guanosine 5'-O-[gamma-thio]triphosphate, ISO- isoproterenol, SYNAC-
Synthetic Adenylyl Cyclase

MOL #101626

ABSTRACT: Adenylyl cyclase (AC) activity relies on multiple effectors acting through distinct binding sites. While crystal structures have revealed the location of these sites and biochemical studies have explored the kinetics of ACs, the interplay between conformation and activity remains incompletely understood. Here, we describe a novel FRET sensor that functions both as a soluble cyclase and a reporter of complementation within the catalytic domain. We report a strong linear correlation between catalytic domain complementation and cyclase activity upon stimulation with forskolin and $G\alpha_s$. Exploiting this, we dissect the mechanism of action of a series of forskolin analogues and a P-site inhibitor, 2'-d3'-AMP. Lastly, we demonstrate that this sensor is functional in live cells, wherein it reports forskolin-stimulated activity of AC.

MOL #101626

INTRODUCTION

Adenylyl cyclases (ACs) catalyze the production of cyclic AMP (cAMP) from cellular ATP. Most ACs are integral membrane proteins with a membrane-tethered catalytic domain formed from a C1 and a C2 domain that have a weak affinity for each other basally ($>10\ \mu\text{M}$), and together have very little activity despite being held in close proximity (Tesmer and Sprang, 1998). These same domains, however, experience an ~ 100 fold increase in affinity and a similar increase in activity when stimulated with effectors such as forskolin and $G\alpha s$ (Tesmer et al., 1997). Though all of these effectors enhance AC activity, they do so through distinct, spatially separated binding sites on the catalytic domain. Crystal structures of the catalytic domain show that the effectors bridge the C1 and C2 domains to varying extents (Tesmer et al., 1997). Hence, the degree to which complementation between C1 and C2 is a limiting step in effector-dependent activation of cyclase remains unclear and is the focus of this study.

Given that C1 and C2 are the minimal domains necessary for the catalytic activity of the cyclase, they have formed the focus of numerous studies examining the regulation of cyclase activity. Several versions of soluble ACs have been engineered by fusing the cytosolic domains (C1 and C2) of a single isoform (homodimer) or different isoforms (heterodimers) (Tang and Gilman, 1995; Dessauer and Gilman, 1996; Scholich et al., 1997). While cyclase fusions have been used to gain insight into effector-dependent regulation of catalytic activity, they have not been leveraged to examine the conformation of the molecule. Here, we engineer a synthetic adenylyl cyclase conformation sensor (SYNAC) using an ER/K linker flanked by a FRET pair within a cyclase fusion to generate. The ER/K linker is a semi-rigid single protein alpha helix (consisting of a repeating sequence of glutamic acid (E) and arginine or lysine (R/K) residues) that separates the two domains beyond FRET range and provides a substantial barrier to non-specific complementation (Sivaramakrishnan et al., 2008). Interactions between the domains flanking the ER/K linker bring the FRET pair in close proximity leading to a measurable increase in FRET

MOL #101626

(Swanson and Sivaramakrishnan, 2014). In addition, effector dependent complementation of the C1 and C2 domains stimulates cAMP generation, which can be measured using established assays. Using these combined advantages, we observed a linear correlation between the affinity of the C1-C2 interaction and activity of the cyclase fusion. By exploiting this phenomenon, we demonstrate that a family of forskolin-derived inhibitors known as deoxyforskolins is incapable of stimulating activity due to their inability to induce complementation. In contrast, while the P-site inhibitor 2'-d3'-AMP stabilizes the complemented conformation it inhibits cyclase activity as it overlaps with the catalytic site. Lastly, we find that the synergistic effects of G α s and forskolin on AC activity also translate to domain complementation, which can be observed in live cells.

MATERIALS AND METHODS

Constructs

Domains from adenylyl cyclase (AC) II and V (*Homo sapiens*) were amplified via PCR from cDNAs acquired from DNASU. SYNAC sensors were encoded as single polypeptide, from N- to C-terminus as ACII C2 (residues 822-1090) -mCerulean-TEV protease site-30 nm ER/K linker-mCitrine-ACV C1a (residues 444-670)-mCitrine-FLAG tag. One to two flexible Gly-Ser-Gly linkers connect all domains (see Supplemental Fig. 1). The long splice variant of G α s (*H. sapiens*) was amplified from cDNA (Open Biosystems) and was cloned between unique restrictions sites with an N-terminal FLAG-tag. β 2AR-His-G α s was generated by restriction enzyme cloning and consists of β 2-AR followed by a 6xHis-tag followed immediately by a full length G α s, replicating the β 2AR-His-G α s fusion construct published by Seifert et al. (Seifert et al., 1998).

MOL #101626

Insect Cell Culture and Protein Purification

Sf9 cells were cultured at 28 °C in Sf900-II medium (Invitrogen) with 1% antibiotic-antimycotic (Invitrogen). Constructs were transiently transfected into Sf9 cells using Escort IV transfection reagent (Sigma-Aldrich) in antibiotic-free medium. For FLAG-tag purification, cells were lysed three days post-transfection in lysis buffer (0.5% IGEPAL, 4 mM MgCl₂, 200 mM NaCl, 7% sucrose, 20 mM HEPES (pH 7.5), 5 mM DTT, 50 µg/ml PMSF, 5 µg/ml aprotinin, 5 µg/ml leupeptin). Lysates were clarified by ultracentrifugation (200,000 × g, 4 °C, 45 min) and bound to anti-FLAG M2 affinity gel (Sigma-Aldrich) at 4 °C. FLAG resin was washed with wash buffer (150 mM KCl, 20 mM HEPES (pH 7.5), 5 mM MgCl₂, 5 mM DTT, 50 µg/ml PMSF, 5 µg/ml aprotinin, 5 µg/ml leupeptin) and eluted overnight using FLAG peptide (Sigma-Aldrich). Gαs was further incubated overnight with either 115 µM GDP or GTPγS (Sigma-Aldrich). SYNAC was desalted using Zeba Spin desalting columns (Pierce) into Assay Buffer (50 mM HEPES (pH 8.0), 50 mM NaCl, 5 mM MgCl₂). Gαs was desalted into the same buffer containing 115 µM GDP or GTPγS. Concentrations of SYNAC were determined by comparison of fluorescence intensity to known standards. Concentrations of Gαs were determined by gel electrophoresis and Coomassie staining compared to known concentration of BSA. Protein integrity was assessed by gel electrophoresis, using fluorescent imaging (Typhoon gel imager; GE Healthcare) and/or Coomassie staining. Additional integrity measurements were possible through the use of TEV protease. Briefly, protein samples were digested with TEV protease at room temperature for 2 hours, run on a 10% SDS-PAGE gel, and fluorescently scanned and/or Coomassie stained as described above to monitor protein fragment size as compared to intact and expected molecular weights.

Fluorometer Data Acquisition

Data were acquired on a FluoroMax-4 fluorometer (Horiba Scientific). FRET spectra were generated by exciting samples at 430 nm (spectral band pass 8 nm) and emission was scanned from 450-650

MOL #101626

nm (band pass 4 nm). All data were taken at an estimated 30 nM SYNAC (based on mCerulean fluorescence; extinction coefficient: $\epsilon 43,000 \text{ M}^{-1}\text{cm}^{-1}$). Measurements were taken in Assay Buffer. All tubes were pre-coated with 0.05 mg/ml BSA for at least 5 minutes to limit non-specific surface adsorption of proteins. This “pre-coat” solution was aspirated before addition of reaction components. For conditions containing forskolin or deoxyforskolin analogues (Sigma-Aldrich), the equivalent controls were matched for concentration of DMSO (forskolin stock 10 mM in 100% DMSO, deoxyforskolin analogues 5 mM in 100% DMSO). Gas was used at a concentration of 800 nM. All FRET ratios are represented as the average of three repeat measurements. For live cell fluorescence spectra, cultured Sf9 cells were harvested between 16 and 24 hours of expression. Cells were counted and resuspended to equal concentration ($\sim 2 \times 10^6$ cells/ml) in HEPES buffered saline (20 mM HEPES (pH 7.4), 5 mM KCl, 14.5 mM NaCl, 2 mM CaCl_2 , 1 mM MgCl_2) with 0.2% dextrose and 1 mM ascorbic acid and measured as described above for fluorescence. Background subtraction was applied using non-transfected cells at the same concentration of cells per milliliter.

Cyclase Activity

The Kinase-Glo Max Assay (Promega) was used to assess cyclase activity through ATP consumption. Briefly, the indicated conditions were pipetted into BSA pre-coated tubes containing an estimated 30 nM SYNAC and 0.05 U inorganic pyrophosphatase (NEB; from *E. coli*). Either 500 μM or 1 mM ATP was added to initiate the reaction. Tubes were incubated at 30 °C for 30 minutes before being divided into 20 μL aliquots and halted with an equal addition of Kinase-Glo Max reagent. For experiments including inorganic pyrophosphate as a condition, samples were not pipetted with pyrophosphatase. Instead, the reaction was halted after 30 minutes by incubation at 65 °C for 15 minutes. Samples were then quickly cooled to room temperature and 0.05 units of pyrophosphatase were added and the samples were incubated at 30 °C for 15 minutes and then processed as normal. ATP

MOL #101626

consumption was measured as luciferase activity as read by a 96-well microplate luminometer (M5e Spectramax spectrophotometer, Molecular Devices).

cAMP Generation

The cAMP-Glo Assay (Promega) was used to assess cyclase activity in live cells. In live cells, Sf9 cells expressing equal amounts of protein were harvested three days post-transfection, collected by centrifugation at 250 x g for 3 min, washed once with HEPES buffered saline with dextrose (see above) and resuspended at equal optical density. Cells were then treated for 10 minutes at room temperature with buffer, 100 μ M isoproterenol (Sigma-Aldrich), or forskolin, and processed according to the manufacturer's instructions. Luminescence was measured using a 96-well microplate luminometer (M5e Spectramax spectrophotometer, Molecular Devices).

Statistical Analysis

All activity data is the average of at least 3 independent repeats using different preparations of protein and error is calculated as \pm SEM. FRET data is the average of at least three spectra and error is calculated as \pm SD. All non-spectra data was plotted and statistically analyzed in Graphpad Prism 6 (Graphpad Software). Spectra data are the average of three repeats and were plotted in Matlab (Mathworks). Where presented unless indicated otherwise, statistical significance is assessed using an unpaired Student's t-test as performed by Graphpad Prism 6.

RESULTS

The domains included in our construct are based on the work of Tesmer et al. (Tesmer et al., 1997) and Hatley et al. (Hatley et al., 2002), and consists of C1a and C2a domains of ACII and ACV, respectively. This "catalytic core" of the C1a and C2a domains of ACs has been demonstrated to have a weak affinity between the two domains ($\sim 10 \mu$ M) and is sufficient to reconstitute cAMP generation

MOL #101626

(Tang and Gilman, 1995). In the SYNAC sensor, these domains are separated by a modular 30 nm ER/K linker that provides weak basal complementation (effective concentration ~ 100 nM) between the domains (Swanson and Sivaramakrishnan, 2014) as well as providing a substantial separation between the two sets of fluorophores used for the FRET readout (Fig. 1a). This allows both halves of the catalytic domain to be expressed at equal stoichiometry and with minimal basal activity, but with robust activation when stimulated with the specific AC-activating small molecule forskolin (FSK; Fig. 1b). Two FRET acceptors (mCitrine) were used with a single FRET donor (mCerulean) as this greatly improved the dynamic range of the FRET sensor (data not shown).

FSK-driven activation of SYNAC is concentration dependent and remains fairly linear up to 300 μ M FSK (Fig. 1b). The lack of saturation of SYNAC activity at high forskolin concentrations is consistent with previous observations with cyclase fusions (Tang and Gilman, 1995). Given that there is a direct 1:1 correlation between cAMP production and ATP metabolism by ACs (Dessauer et al., 1996), SYNAC activity can be easily monitored indirectly by ATP metabolism through a coupled luciferase assay. However, due to the production of pyrophosphate - a potent inhibitor of luciferase activity (Supplemental Fig. 2a) - during the cyclization reaction, luminescence varies non-linearly with residual ATP concentration. Addition of inorganic pyrophosphatase metabolizes pyrophosphate into phosphate, which does not interfere with luciferase activity. The incorporation of pyrophosphatase is sufficient to rectify this loss of luminescence and render a linear correlation between luminescence and residual ATP concentration (Supplemental Fig. 2b, See Methods).

FRET between the fluorophores mCerulean (mCer) and mCitrine (mCit) flanking the ER/K linker allows us to monitor the fraction of SYNAC in the closed conformation (Fig. 1c) (Sivaramakrishnan and Spudich, 2011). FRET response is directly proportional to activity, indicating that a closed conformation of SYNAC, wherein the two domains are in close proximity, has much greater activity than the

MOL #101626

open or low FRET conformation (Fig. 1d). This strongly supports the conclusions of Tesmer et al. (Tesmer et al., 1997) drawn from the crystal structure of adenylyl cyclase.

To further explore the relationship between conformation and activity, we investigated a number of forskolin analogues that are known competitive inhibitors of ACs. These inhibitors, known as deoxyforskolins (dFSKs), lack an oxygen atom at various places on the diterpene rings of forskolin and compete for the same binding site as FSK. Interestingly, when incubated with SYNAC, some of these dFSK compounds were still able to induce modest activity, albeit requiring much higher concentrations and to a far lower extent than FSK (Fig. 2 a-c). Further, when FRET was monitored, increasing concentrations of dFSK compounds corresponded with increased levels of FRET (Fig. 2d). Notably, the behavior of SYNAC in the presence of these dFSK compounds followed our observation of a linear correlation between activity and FRET (conformation) with FSK (Fig. 2e). In order to test that these dFSK compounds were indeed capable of inhibiting FSK-stimulated activity, SYNAC was stimulated with 10 μ M FSK under increasing concentrations of 1-dFSK (Fig. 2f). A reduction in the observed activity was visible at a high concentration of 1-dFSK and a similar drop in FRET was also observed (Supplemental Fig. 3). This suggests that 1-dFSK does bind SYNAC, albeit more weakly, and therefore is not as efficient at complementing the AC catalytic domain.

2'-d3'-AMP belongs to a class of uncompetitive inhibitors known as "P-site" inhibitors that have been shown to inhibit AC activity by occupying the ATP binding pocket along with pyrophosphate, prohibiting the enzyme from interacting with ATP (Dessauer and Gilman, 1997; Dessauer et al., 1999). Due to the low basal activity of SYNAC, SYNAC must first be stimulated to observe inhibition. Accordingly, SYNAC stimulated with FSK showed a significant decrease in activity when both 2'-d3'-AMP and pyrophosphate were present (Fig. 3a). It must be noted that the 2'-d3'-AMP condition also contains residual pyrophosphate generated during cAMP synthesis that can enhance 2'-d3'-AMP bind-

MOL #101626

ing (see Methods). This likely contributes to the suppression of SYNAC activity with 2'-d3'-AMP alone. Counterintuitively, the domain complementation in SYNAC, as measured by FRET is further increased above the previous maxima of 100 μ M FSK, in the presence of both pyrophosphate and 2'-d3'-AMP (stimulated with 100 μ M FSK, Fig. 3b). Our results suggest that a complemented state of the enzyme is being strongly stabilized by the presence of the inhibitor and pyrophosphate; hence its use in the crystal structure published by Tesmer et al. (Tesmer et al, 1997). ATP also facilitates complementation (increase in FRET), but does not provide an increase above the stimulated maxima at 100 μ M FSK, suggesting that the ATP bound state is more transient in the FSK stimulated conformation (Fig. 3b). The addition of pyrophosphate to the reaction by itself does not have a significant effect on either cyclase activity or FRET (Fig 3a,b).

Besides FSK, the other canonical activator of ACs is the G α s subunit. SYNAC displayed a synergistic increase in activity selectively with GTP γ S bound G α s (Fig. 4a). Following previous trends in our data, this correlated with an increase in FRET for GTP γ S bound G α S incubated with SYNAC alone and a substantial increase in FRET when incubated with both FSK and GTP γ S bound G α s (Fig. 4b). The synergistic effects of FSK treatment and GTP γ S bound G α s were also visible when monitoring FRET (Fig. 4c). Notably, SYNAC reported a modest increase in FRET and activity when stimulated with GDP-bound G α s, which has been reported as possessing a 10-fold lower affinity for cyclase (Sunahara et al., 1997).

Traditionally, insect (Sf9) cells have been used as a platform for probing GPCR-G protein interactions and G protein-AC interactions due to the apparent lack of interference from endogenous G proteins (Schneider and Seifert, 2010). When SYNAC was expressed in Sf9 cells and stimulated with FSK, we were able to observe AC activity above endogenous levels (Fig. 5a). SYNAC displayed enhanced basal cAMP production when cells were co-transfected with G α s (Fig. 5b). Further, when SYNAC was

MOL #101626

co-expressed with a $\beta 2$ -AR- $G\alpha s$ fusion protein (similar to that previously used by Seifert et al. (Seifert et al. 1998)), we observed both basal and isoproterenol-stimulated cAMP production (Fig. 5c). Although, cAMP levels were detected to be much higher than basal levels when coexpressed with the $\beta 2$ -AR- $G\alpha s$, this is likely due to the increased activity of SYNAC basally in the presence of $G\alpha s$ (Fig. 5b). In spite of this increased basal activity, we are still able to see a statistically significant increase in signal from isoproterenol addition. However, inconsistent with the lack of any observable basal activity, SYNAC expressed alone in live cells had high basal FRET levels, but showed a significant increase in FRET ratio when stimulated with 100 μ M forskolin (Fig. 5d). Further, cells coexpressing SYNAC with $G\alpha s$ or the $\beta 2$ -AR- $G\alpha s$ fusion showed elevated basal levels of FRET as compared to SYNAC alone and $\beta 2$ -AR- $G\alpha s$ showed a further increase over $G\alpha s$ alone with SYNAC (Fig. 5d). The elevated FRET levels are consistent with high basal cAMP generation in live cells. Isoproterenol stimulation leads to a small, but statistically significant increase above already high levels of cAMP (Fig 5c). However, the corresponding FRET response was insignificant (Fig 5d). This is unsurprising, considering the already high levels of FRET and the incremental effect in cAMP generation. Overall, our sensor effectively recapitulates the activity state of cyclase in live cells.

DISCUSSION

In this study a FRET-based biosensor, termed SYNAC, was used to demonstrate a linear correlation between catalytic domain complementation and enzymatic activity in adenylyl cyclase. FRET-based biosensors have been used extensively to monitor AC activity in live cells. These AKAR sensors (Zhang et al., 2001) have been instrumental in mapping the spatio-temporal regulation of cAMP in response to a range of stimuli. However, they are designed to track cAMP generation rather than cyclase conformation. Also, while catalytic domain fusions of AC have previously been used to understand effector-dependent regulation of cyclase activity, they have not been engineered to probe the confor-

MOL #101626

mation of the molecule. The combination of using a cyclase fusion and a FRET-based detection system addresses the questions of cyclase conformation and enzymatic activity using a single construct.

SYNAC is capable of integrating information from activity and conformation. Using this advantage, our data suggest that even though the two catalytic domains are held in relative proximity to each other at the plasma membrane, the increase in affinity triggered by effector binding is necessary for cyclase activity. This correlation between affinity and activity also provides us with insight into the mechanisms of forskolin and deoxyforskolin action. Forskolin binds cyclase relatively weakly in the absence of GαS as witnessed by a lack of saturation of both activity and catalytic domain complementation at concentrations approaching its solubility limit (Fig. 1b) (Tang and Gilman, 1995). The presence of GαS substantially increases the ability of FSK to complement and activate the cyclase (Fig. 4b). dFSKs lack oxygens at C-1 and/or C-9 positions on the FSK diterpene ring, both of which are important elements of the FSK-binding interface (Tesmer et al., 1997). The absence of these oxygens disrupts catalytic domain complementation and, consequently, activity as well (Fig. 2a-e). In addition, dFSKs bind SYNAC weakly as reflected in the substantially higher concentrations required to inhibit FSK stimulated SYNAC (Fig. 2f). Of note, however, is that the oxygen in the C-1 position on the diterpene ring appears to be more important for activity than the oxygen in the C-9 position, given the higher activity and complementation observed with 9-dFSK as compared to 1-dFSK (Fig. 2a,b,d). Further, as illustrated by 2'-d3'-AMP, an increase in affinity is not always correlated with an increase in activity (Fig. 3 a,b). Instead, by occupying the active site, molecules such as 2'-d3'-AMP trap the cyclase in what would ordinarily appear to be an active conformation, based on complementation alone, but is actually catalytically silent. Hence, a two-pronged approach of monitoring both cyclase conformation and cAMP generation using SYNAC can provide additional information on the mechanism of drug action in ACs.

Cyclase activation stems from a combination of catalytic domain complementation and allosteric changes in the catalytic domain that lead to a catalytically competent enzyme. SYNAC was engineered

MOL #101626

with a long structural ER/K linker flanked by a FRET pair to examine domain complementation in the context of enzymatic activity. Nonetheless, the inclusion of exogenous elements can alter interactions within the catalytic domain to influence the kinetics of this enzyme. Further, it is unclear to what extent the two halves of the catalytic domain are in proximity to each other in the native enzyme. Hence, it is possible that the catalytic domain is basally well-complemented in the full length molecule. In this context, activation of the enzyme in response to effectors would stem primarily from subtle conformational changes that mirror the observed changes in domain complementation. Lastly, the synthetic nature of the cyclase may influence its behavior in live cells. Contrary to the other findings reported in this work, there is an unexpectedly high level of FRET inside live cells in spite of a low level of basal activity (Fig. 5a,d). There are multiple factors that could contribute to this higher basal FRET, including clustering at the membrane, compartmentalization of the overexpressed protein, and interactions with other uncharacterized modulators of cyclase conformation. However, SYNAC does retain its sensitivity to effectors and further studies are necessary to interpret measurements in live cells.

AUTHORSHIP CONTRIBUTIONS

Participated in research design: Ritt and Sivaramakrishnan.

Conducted experiments: Ritt.

Performed data analysis: Ritt and Sivaramakrishnan.

Wrote or contributed to the writing of the manuscript: Ritt and Sivaramakrishnan.

MOL #101626

REFERENCES

- Dessauer CW, Gilman AG (1996) Purification and characterization of a soluble form of mammalian adenylyl cyclase. *J Biol Chem* 271(28):16967-16974
- Dessauer CW, Gilman AG (1997) The catalytic mechanism of mammalian adenylyl cyclase. Equilibrium binding and kinetic analysis of P-site inhibition. *J Biol Chem* 272(44):27787-27795
- Dessauer CW, Tesmer JJ, Sprang SR, Gilman AG (1999) The Interactions of adenylate cyclases with P-site inhibitors. *Trends in Pharmacol Sci* 20(5):205-210
- Hatley ME, Gilman AG, Sunahara RK (2002) Expression, purification, and assay of cytosolic (catalytic) domains of membrane-bound mammalian adenylyl cyclases. *Methods Enzymol* (345):127-140
- Schneider EH, Seifert R (2010) Sf9 cells: a versatile model system to investigate the pharmacological properties of G protein-coupled receptors. *Pharmacol Ther* 128(3):387-418
- Scholic K, Barbier AJ, Mullenix JB, Patel TB (1997) Characterization of soluble forms of nonchimeric type V adenylyl cyclases. *Proc Natl Acad Sci* 94(7):2915-2920
- Seifert R, Lee TW, Lam VT, Kobilka BK (1998) Reconstitution of beta2-adrenoceptor-GTP-binding protein interaction in Sf9 cells--high coupling efficiency in a beta2-adrenoceptor-G(s alpha) fusion protein. *Eur J Biochem* 255(2):369-382
- Sivaramakrishnan S, Spudich JA (2011) Systematic control of protein interaction using a modular ER/K α -helix linker. *Proc Natl Acad Sci* 108(51):20467-20472
- Sivaramakrishnan S, Spink BJ, Sim AY, Doniach S, Spudich JA (2008) Dynamic charge interactions create surprising rigidity in the ER/K alpha-helical protein motif. *Proc Natl Acad Sci* 105(36):13356-13361
- Sunahara RK, Dessauer CW, Whisnant RE, Kleuss C, Gilman AG (1997) Interaction of Gsa with the cytosolic domains of mammalian adenylyl cyclase. *J Biol Chem* 272(35):22265-22271
- Swanson CJ, Sivaramakrishnan S (2014) Harnessing the unique structural properties of isolated alpha-helices. *J Biol Chem* 289(37):25460-25467
- Tang WJ, Gilman AG (1995) Construction of a soluble adenylyl cyclase activated by Gs alpha and forskolin. *Science* 268(5218):1769-1772
- Tesmer JJ, Sprang SR (1998) The structure, catalytic mechanism and regulation of adenylyl cyclase. *Curr Opin Struct Biol* 8(6):713-719
- Tesmer JJ, Sunahara RK, Gilman AG, Sprang SR (1997) Crystal structure of the catalytic domains of adenylyl cyclase in a complex with Gsalpha.GTPgammaS. *Science* 278(5345):1907-1916

MOL #101626

Zhang J, Ma Y, Taylor SS, Tsien RY (2001) Genetically encoded reporters of protein kinase A activity reveal impact of substrate tethering. 98(26):14997-15002

FOOTNOTES

This work was supported by the NIH [Grants 1DP2 CA186752-01, 1-R01-GM-105646-01-A1]; the AHA SDG Award [Grant 13SDG14270009], to S.S.

MOL #101626

FIGURE LEGENDS

Fig. 1. Characterization of synthetic adenylyl cyclase (SYNAC). (A) Schematic diagram of SYNAC. Black dashed line indicates TEV protease cleavage site. Schematic shows the expected complementation of the ACII-C2 and ACV-C1 domains following stimulation with activated G α S (GTP γ S) or forskolin (FSK). (B) SYNAC displays FSK-stimulated activity in a concentration dependent fashion. Activity is measured in terms of ATP metabolized by SYNAC. Inset is the structure of forskolin. Data is mean \pm SEM of three independent repeats using three different preparations of protein. (C) FSK stimulates domain complementation in SYNAC. Normalized fluorescence emission spectrum (mCerulean, Excitation 430 nm) of SYNAC stimulated with the indicated concentrations of FSK. Data is average of 3 repeats. (D) FRET of SYNAC (mCit/mCer; 525 nm/475 nm) plotted against activity at the indicated concentrations of the compound. R^2 of 0.93 indicates a linear relationship between the two parameters. Activity data is mean \pm SEM of three independent repeats using three different preparations of protein. FRET data is mean \pm SD of three spectra. Spectra are presented as mean without error bars for clarity.

Fig. 2. Deoxyforskolin-stimulated complementation in SYNAC correlates with activity. (A-C) Effects of the indicated deoxyforskolin (dFSK) molecule on SYNAC activity. Insets represent structure of the indicated dFSK molecule with red boxes indicating differences from the structure of FSK. (D) Effects of the indicated dFSK molecules on SYNAC FRET at the indicated concentrations. (E) Activity of SYNAC plotted against FRET readout at 100 μ M of the indicated compound. R^2 of 0.94 indicates a highly linear correlation. (F) Inhibition of 10 μ M FSK stimulated SYNAC activity by 1-dFSK at the

MOL #101626

indicated concentrations. The red line indicates basal activity levels for SYNAC. The solid black line indicates 10 μ M FSK stimulated SYNAC activity with the dashed lines representing standard error (SEM). Data for this panel was normalized to forskolin-stimulated activity and significance was assessed by Student's t-test (paired) to account for a systematic bias in data. Activity data is mean \pm SEM of three independent repeats using three different preparations of protein. FRET data is mean \pm SD of three spectra. Significance assessed by Student's t-test (unpaired) unless otherwise indicated. *** = $p < 0.001$.

Fig. 3. 2'-d3'-AMP stimulates complementation in SYNAC without stimulating activity. (A) Effects of either 100 μ M 2'-d3'-AMP, 100 μ M pyrophosphate (PPi), or both together (as indicated) on SYNAC activity in the presence of 100 μ M FSK. PPi is being generated from FSK-stimulated SYNAC activity and inhibits cyclase activity in conjunction with 2'-d3'-AMP. In this assay, pyrophosphatase was added after the reaction had been stopped by denaturation at 65 °C to remove pyrophosphate from solution, allowing detection by luciferase (see Methods). (B) The effects of 2'-d3'-AMP, ATP, and PPi on SYNAC FRET in the presence and absence of 100 μ M FSK. Counterintuitively, the FRET detected in the presence of both 2'-d3'-AMP and PPi increases. Activity data is mean \pm SEM of three independent repeats using three different preparations of protein. FRET data is mean \pm SD of three spectra. Significance assessed by Student's t-test (unpaired). n.s. = not significant, * = $p < 0.05$, ** = $p < 0.01$.

Fig. 4. G α s stimulates SYNAC synergistically with FSK in a GTP-dependent manner. (A) FSK and G α s synergistically stimulate SYNAC in a GTP-dependent manner. SYNAC was stimulated with 200 nM G α s bound either to GDP or GTP γ S at the indicated concentrations of FSK. (B) Complementation

MOL #101626

of SYNAC domains is enhanced by GTP-bound $G\alpha_s$. FRET response of SYNAC stimulated with 200 nM $G\alpha_s$ bound either to GDP or GTP γ S, with or without 1 μ M FSK. **(C)** Complementation of SYNAC domains is synergistic to GTP- $G\alpha_s$ and FSK. FRET response of SYNAC with or without GTP γ S bound $G\alpha_s$ (800 nM), in the presence of the indicated concentrations of FSK. Activity data is mean \pm SEM of three independent repeats using three different preparations of protein (both SYNAC and $G\alpha_s$). FRET data is mean \pm SD of three spectra. Significance assessed by Student's t-test (unpaired). n.s. = not significant, * = $p < 0.05$, ** = $p < 0.01$, *** = $p < 0.001$, **** = $p < 0.0001$

Fig. 5. Effector stimulated activity of SYNAC in live cells. **(A)** cAMP generation in untransfected (Sf9) or SYNAC expressing Sf9 cells (SYNAC) following treatment with indicated concentrations of FSK. cAMP levels are reported relative to untransfected, untreated cells. **(B)** Basal cAMP levels are elevated in Sf9 cells co-expressing SYNAC and $G\alpha_s$, but not SYNAC or $G\alpha_s$ independently. **(C)** cAMP levels are basally elevated in cells co-expressing SYNAC and a β 2-AR- $G\alpha_s$ fusion protein, and are further increased by addition of isoproterenol (ISO). cAMP levels in Sf9 cells expressing SYNAC, β 2-AR- $G\alpha_s$ fusion, or coexpressing SYNAC and β 2-AR- $G\alpha_s$ fusion with or without 100 μ M ISO treatment (10 min). **(D)** SYNAC FRET response in Sf9 cells following FSK (100 μ M) and ISO (100 μ M) treatment with and without coexpression of $G\alpha_s$ and β 2-AR- $G\alpha_s$. Both conditions were incubated for 5 minutes with their respective conditions. Cells were held at equivalent OD and expression as judged by mCerulean fluorescence. Activity data is mean \pm SEM of three independent repeats using three different preparations of protein. FRET data is mean \pm SD of four spectra. Significance assessed by Student's t-test (unpaired). n.s. = not significant, ** = $p < 0.01$, *** = $p < 0.001$, **** = $p < 0.0001$

FIGURE 1

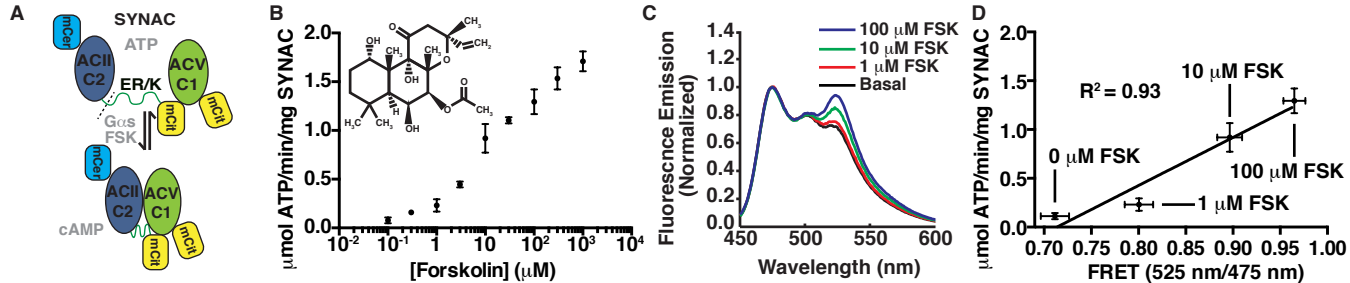


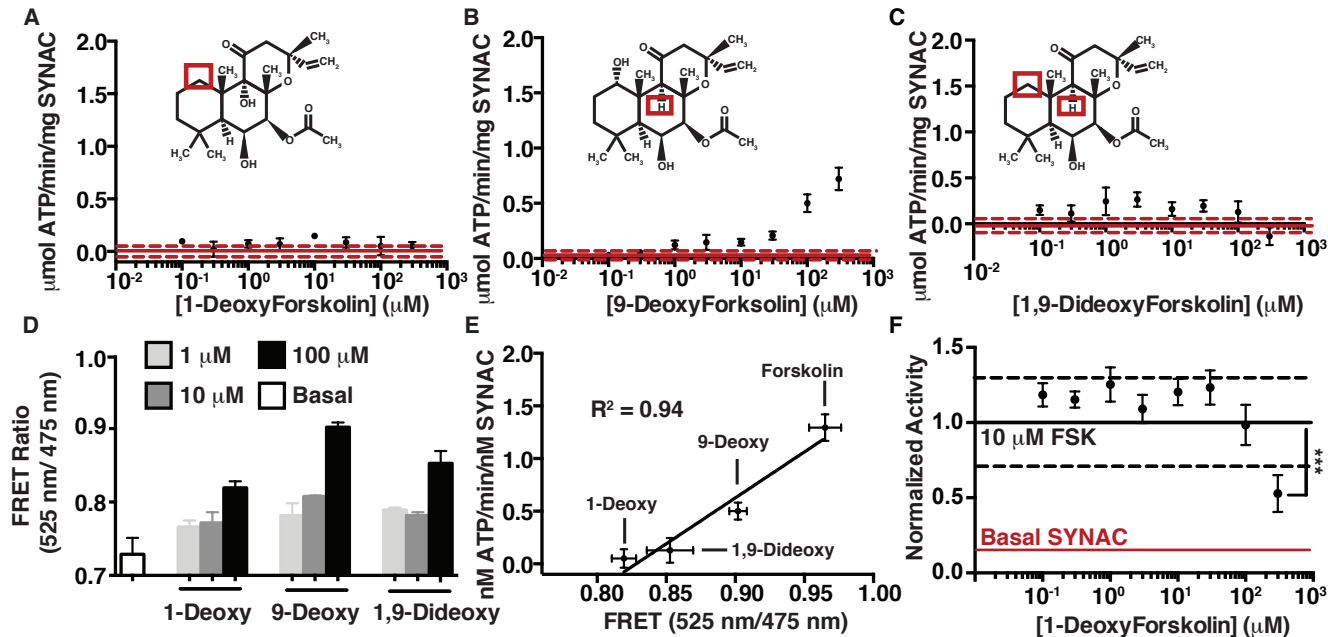
FIGURE 2

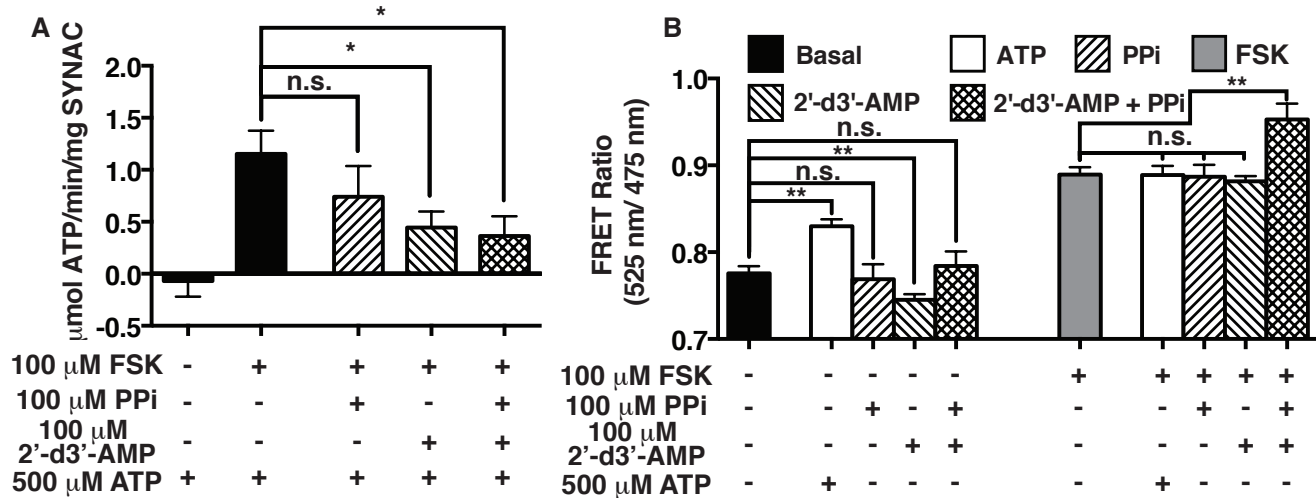
FIGURE 3

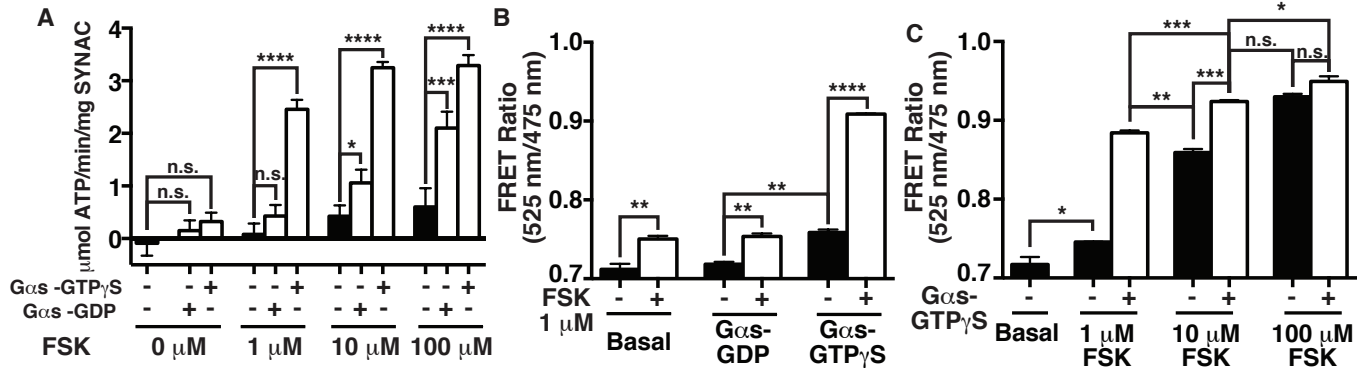
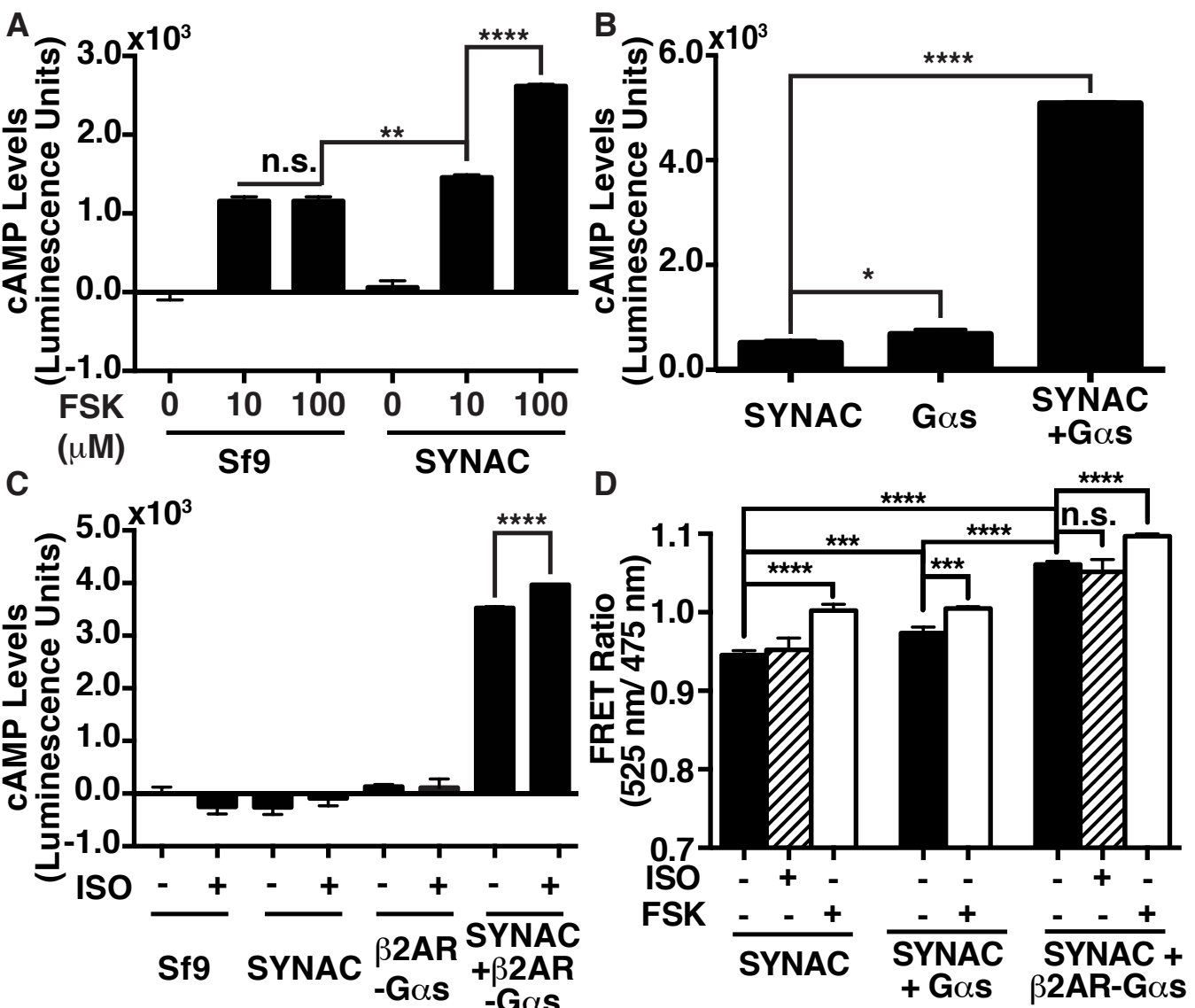
FIGURE 4

FIGURE 5



Correlation between activity and domain complementation in adenylyl cyclase
demonstrated with a novel FRET sensor
Michael Ritt, Sivaraj Sivaramakrishnan
Molecular Pharmacology

Supplementary Figure 1- Sequence and domain organization of SYNAC

Amino Acid Sequence of SYNAC

MG**TM**MQNEYCYRLDFLWKNKFKKEREEIETMENLNRVLLENVLPAHVAEHFLARSLKN
EELYHQSYDCVCVMFASIPDFKEFYTESDVNKEGLECLRLLNEIIADFDDLLSKPKFSGVEK
IKTIGSTYMAATGLSAVPSQEHSQEPERQYMHIGTMVEFAFALVGKLDANKHSFNDFKLR
VGINHGPVIAGVIGAQKPQYDIWGNTVNVASRMDSTGVLDKIQVTEETSLVLQTLGYTCTC
RGIINVKGKGD~~L~~KTYFVNTEMSRSLSSQSNVAS**GSGTSGSG**VSKGEELFTGVVPILVELDGDV
NGHKFSVSGEGEGDATYGKLT**L**KFICTTGKLPVPWPTLVTTLTWGVQCFARYPDHMKQH
DFFKSAMPEGYVQERTIFFKDDGNYKTRAEVKFEGDTLVNRIELKGIDFKEDGNILGHKLE
YNAISDNVYITADKQKNGIKANFKIRHNIEDGSVQLADHYQQNTPIGDGPVLLPDNHYLST
QSKLSKDPNEKRDHMLLEFVTAAGITLGMDELYK**EF****GSGGSG**ENLYFQ**GSG**EEEEKKK
EEEEKKQKEEQERLAKEEAERKQKEEQERLAKEEAERKQKEEEERKQKEEEERKQKEEE
ERKLKEEQERKAAEEKKAKEEAERKAKEEQERKAAEEERKKKEEEERLERERKEREEQEK
KAKEEAERIAKLEAEKKAEEERKAKEEEERKAKEEEERKKKEEQERLAKEEEAERKAAE
EKKAKEEQERKEKEEAERKQR**GSGGSG****GAP**VSKGEELFTGVVPILVELDGDVNGHKFSVS
GEGEGDATYGKLT**L**KFICTTGKLPVPWPTLVTTTFGYGLMCFARYPDHMKQHDFFKSAMP
EGYVQERTIFFKDDGNYKTRAEVKFEGDTLVNRIELKGIDFKEDGNILGHKLEYNYNSHN
YIMADKQKNGIKVNFKIRHNIEDGSVQLADHYQQNTPIGDGPVLLPDNHYLSYQSKLSKDP
NEKRDHMLLEFVTAAGITLGMDELYK**GSGGS****GAP**MEMKADINAKQEDMMFHKIYIQKH
DNVSILFADIEGFTSLASQCTAQELVMTLNELFARFDKLAENHCLRIKILGDCYYCVSGLP
EARADHAHCCVEMGMDMIEAISLVREVTGVNVNMRVGIHSGRVHCGVLGLRKWQFDVW
SNDVTLANHMEAGGKAGRIHITKATLNYLNGDYEVPEPGCGGERNAYLKEHSIETFLILRCT
QKRKEEKAMIAKMNRQRTNSI**VD****GSGGSG**VSKGEELFTGVVPILVELDGDVNGHKFSVSG
EGEGDATYGKLT**L**KFICTTGKLPVPWPTLVTTTFGYGLMCFARYPDHMKQHDFFKSAMP
GYVQERTIFFKDDGNYKTRAEVKFEGDTLVNRIELKGIDFKEDGNILGHKLEYNYNSHN
YIMADKQKNGIKVNFKIRHNIEDGSVQLADHYQQNTPIGDGPVLLPDNHYLSYQSKLSKDP
NEKRDHMLLEFVTAAGITLGMDELYK**GSG****DYKDDDK***

Nucleotide Sequence of SYNAC

Methionine-Glycine

Atg gga

AgeI

aCCGGT

ACII-C2a (*H. sapiens*, aa 823-1083)

ATGCAGAATGAATATTACTGTAGGTTAGACTTCTTATGGAAGAACAAATTCAAAAAAGA
GCGGGAGGAGATAGAGACCATGGAGAACCTGAACCGCGTGCTGCTGGAGAACGTGCTTCC
CGCGCACGTGGCTGAGCACTTCCTGGCCAGGAGCCTGAAGAATGAGGAGCTATACCACCA
GTCCTATGACTGCGTCTGTGTCATGTTTGCCTCCATTCCGGATTTCAAAGAATTTTATAC
AGAATCCGACGTGAACAAGGAGGGCTTGAATGCCTTCGGCTCCTGAACGAGATCATCGC
TGACTTTGATGATCTTCTTTCCAAGCCAAAATTCAGTGGAGTTGAAAAGATTAAGACCA
TTGGCAGCACATACATGGCAGCAACAGGTCTGAGCGCTGTGCCCAGCCAGGAGCACTCCC
AGGAGCCCCGAGCGGCAGTACATGCACATTGGCACCATGGTGGAGTTTGGCTTTTGCCTGG
TAGGGAAGCTGGATGCCATCAACAAGCACTCCTTCAACGACTTCAAATTGCGAGTGGGTA
TTAACCATGGACCTGTGATAGCTGGTGTGATTGGAGCTCAGAAGCCACAATATGATATC
TGGGGCAACACTGTCAATGTGGCCAGTAGGATGGACAGCACCGGAGTCCTGGACAAAAT
ACAGGTTACCGAGGAGACGAGCCTCGTCCTGCAGACCCTCGGATACACGTGCACCTGTCG
AGGAATAATCAACGTGAAAGGAAAGGGGGACCTGAAGACGTACTTTGTAAACACAGAAA
TGTCAAGGTCCCTTTCCCAGAGCAACGTGGCATCC

Glycine-Serine-Glycine linker

GGAAGCGGA

SpeI

actagt

Gly-Ser-Gly linker

GGAAGCGGA

mCerulean

gtgagcaagggcgaggagctgttcaccggggtggtgcccatcctggtcgagctggacggcgacgtaaaccggccacaag
ttcagcgtgtccggcgagggcgagggcgatgccacctacggcaagctgacctgaagttcatctgcaccaccggcaagc
tgcccggtgccctggcccaccctcgtagaccacctgacctggggcggtgcagtgttcgcccgtaccccgaccacatgaag
cagcacgacttcttcaagtccgcatgcccgaaggctacgtccaggagcgaccatcttcttcaaggacgacggcaacta
caagacccgcgcgaggtgaagttcgagggcgacaccctggtgaaccgcatcgagctgaagggcatcgacttcaagga
ggacgggaacatcctggggcacaagctggagtacaacgccatcagcgacaacgtctatatcaccgccgacaagcagaa
gaacggcatcaaggccaacttcaagatccgccacaacatcgaggacggcgagcgtgcagctcgccgaccactaccagca
gaacacccccatcggcgacggccccgt
cccaacgagaagcgcgatcacatggtcctgt
caAG

EcoRI

GAATTC

Gly-Ser-Gly x2

GGAAGCGGAGGAAGCGGA

TEV Protease site

GAAAACCTGTATTTTCAG

Gly-Gly-Ser-Gly linker

GGCGGAAGCGGA

ER/K linker (30 nm)

GAAGAGGAAGAGAAGAAGAAAGAAGAGGAAGAAAAGAAACAAAAAGAAGAACAAGAAA
GACTTGC AAAAGAAGAGGCAGAGAGAAAACAAAAAGAAGAACAAAGAAAGACTTGC AAA
AGAAGAGGCAGAGAGAGAAAACAAAAGGAGGAAGAAGAGAGAGAAAACAAAAGGAAGAAGAA
GAGAGAAAACAAAAGGAGGAAGAAGAAGAAAATTAAAGGAGGAACAAGAAAGAAAAG
CTGCAGAAAGAAAAGAAAGCTAAAGAAGAAGCTGAGAGAAAGGCTAAAGAAGAACAAGA
AAGGAAAGCTGAAGAAGAGAGAAAAGAAGAAAGAAGAGGAAGAAAGACTTGAAAGAGAA
AGAAAAGAGAGAGAAGAACAAGAAAAGAAAGCCAAAGAAGAGGCAGAGAGAATTGCAA
AGTTAGAGGCTGAAAAGAAGGCAGAAAGAAGAAAAGCCAAAGAAGAAGAAGAGAG
AAAAGCCAAAGAAGAAGAGGAAAGAAAGAAGAAAGAGGAGCAAGAAAGACTTGC AAA
GAAAAGGAAGAAGCAGAAAGAAAAGCTGCAGAGGAAAAGAAAGCTAAAGAAGAACAAG
AAAGAAAAGAAAAGGAAGAAGCAGAAAGAAAACAAAGA

Gly-Ser-Gly linker x2

GGCTCTGGCGGCTCTGGC

AscI

Base added for frame shift

GGCGCGCC C

mCitrine

gtgagcaagggcgaggagctgttcaccgggggtggtgcccatcctggtcgagctggacggcgacgtaaacggccacaag
ttcagcgtgtccggcgagggcgagggcgatgccacctacggcaagctgacctgaagttcatctgcaccaccggcaagc
tgcccgtgccctggcccaccctcgtgaccaccttcggctacggcctgatgtgcttcgccgctaccccgaccatgaagc
agcacgacttctcaagtccgcatgccgaaggctacgtccaggagcgcaccatcttcttcaaggacgacggcaactac
aagaccgcgccgaggtgaagttcgagggcgacacctggtgaaccgcatcgagctgaagggcatcgacttcaaggag
gacggcaacatcctggggcacaagctggagtacaactacaacagccacaacgtctatatcatggccgacaagcagaag
aacggcatcaaggtgaacttcaagatccgccacaacatcgaggacggcagcgtgcagctcgccgaccactaccgacg
aacacccccatcggcgacggccccgtgctgctgccgacaaccactacctgagctaccagtccaaactgagcaaaagacc
ccaacgagaagcgcatcacatggctcgtggtgagttcgtgaccgccgcccgggatcactctcggcatggacgagctgtac
aag

Gly-Ser-Gly linker x2

ggcagtggtggatca

AscI Base added for frame shift

ggCGCGCC C

ACV-C1a (*H. sapiens*, aa 442-667)

ATGGAGATGAAAGCAGACATCAACGCCAAGCAGGAGGATATGATGTTCCATAAGATTTA
CATCCAGAAACATGACAACGTGAGCATCCTGTTTGCTGACATCGAGGGCTTCACCAGCCT
GGCGTCCCAGTGCCTGCACAGGAACTGGTCATGACCCTCAACGAGCTCTTCGCCCCTT
TGACAAGCTGGCCGCAGAGAATCACTGTTTACGTATTAAGATCCTTGGGGATTGTTATT
ACTGCGTCTCGGGCTGCCTGAAGCAAGGGCTGACCACGCCCACTGCTGTGTGGAGATGG
GCATGGACATGATCGAGGCCATCTCGTTGGTCCGGGAGGTGACAGGGGTGAACGTGAAC
ATGCGTGTGGGAATTACAGCGGGCGAGTACACTGCGGTGTCCTTGGTCTCAGGAAGTGG
CAGTTCGACGTCTGGTCTAACGATGTACAGCTAGCCAACCACATGGAGGCTGGCGGCAAG
GCAGGACGCATCCACATCACCAGGCTACACTCAACTACCTGAATGGGGACTACGAGGTG
GAGCCAGGCTGTGGGGGCGAGCGCAACGCCTACCTCAAGGAGCACAGTATCGAGACCTTC
CTCATCCTGCGCTGCACCCAGAAGCGGAAAGAAGAGAAGGCCATGATCGCCAAGATGAAC
CGCCAGAGAACCAACTCCATC

Sall

GTCGAC

Gly-Ser-Gly linker x2

ggaagcgggGGCTCTGGC

mCitrine

gtgagcaagggcgaggagctgttcaccggggtggtgcccatcctggtcgagctggacggcgacgtaaaccggccacaag
ttcagcgtgtccggcgagggcgagggcgatgccacctacggcaagctgaccctgaagttcatctgcaccaccggcaagc
tgcccgctgccctggcccaccctcgtgaccaccttcggctacggcctgatgtgcttcgccgctaccccgaccacatgaagc
agcacgacttcttcaagtccgcatgccgaaggctacgtccaggagcgcaccatcttcttcaaggacgacggcaactac
aagaccgcgcccaggtgaagttcgagggcgacaccctggtgaaccgcatcgagctgaagggcatcgacttcaaggag
gacggcaacatcctggggcacaagctggagtacaactacaacgccacaacgtctatatcatggccgacaagcagaag
aacggcatcaaggtgaacttcaagatccgccacaacatcgaggacggcagcgtgcagctcgccgaccactaccagcag
aacacccccatcggcgacggccccgtgctgctgcccgacaaccactacctgagctaccagtccaaactgagcaaagacc
ccaacgagaagcgcgatcacatgggtcctgctggagttcgtgaccgccgcccgggatcactctcggcatggacgagctgtac
aag

Gly-Ser-Gly linker

ggaagcggg

FLAG tag

GACTACAAGGACGATGACGACAAG

Stop NotI

TGA GCggccgc

Supplementary Figure 1- Sequence and domain organization of SYNAC

Amino acid and DNA sequences of SYNAC. Colors of domains correlate between the DNA sequence and the protein sequence. Briefly, the methionine and stop codons are uncolored, restriction sites used for cloning are colored red, the adenylyl cyclase II c2 domain is colored cyan, glycine-serine-glycine linkers are magenta, mCerulean is navy blue, the TEV site is colored grey, the ER/K linker is colored dark teal, mCitrine is yellow, adenylyl cyclase V c1 domain is colored green, and the FLAG tag is colored brown.

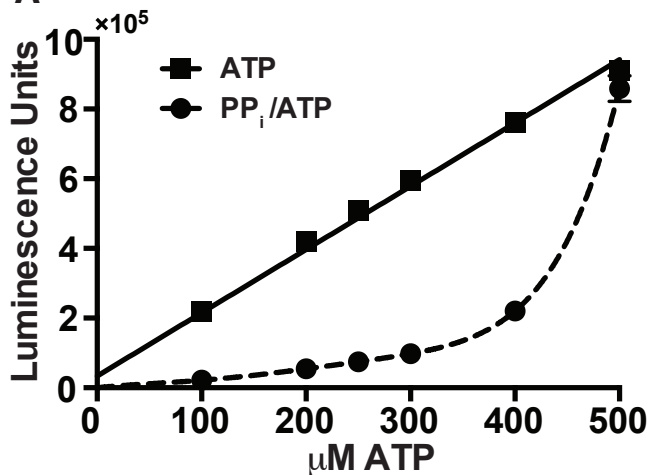
SUPPLEMENTAL FIGURE 2

Correlation between activity and domain complementation in adenylyl cyclase demonstrated with a novel FRET sensor

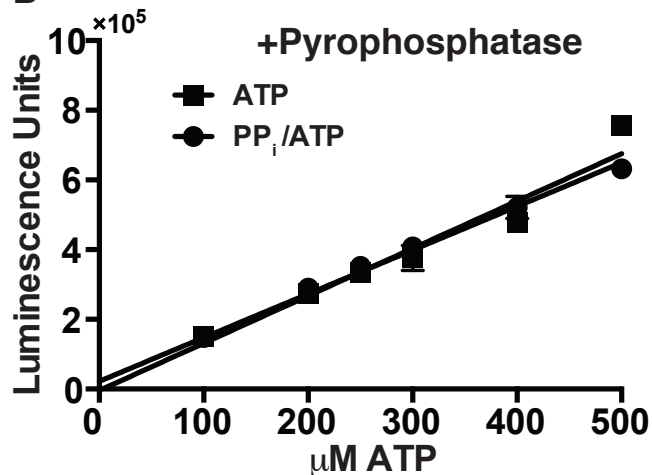
Ritt, Sivaramakrishnan

Molecular Pharmacology

A



B



Supplementary Fig. 2. Luciferase inhibition by pyrophosphate.

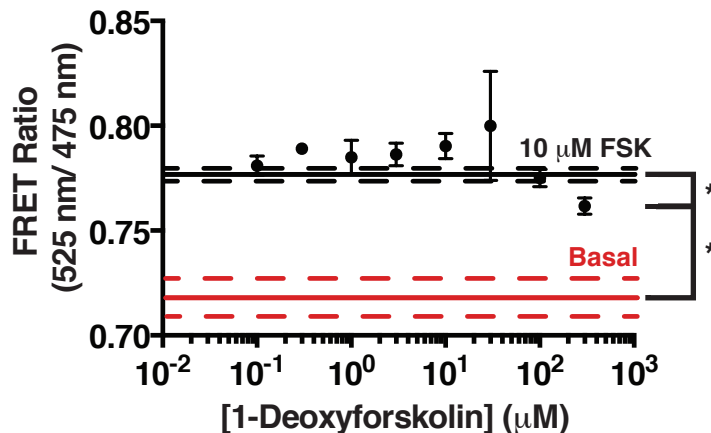
(A) Pyrophosphate inhibits luciferase activity. Squares (solid line) show luminescence in terms of ATP concentration. Circles (dashed line) show luminescence in terms of ATP with a balance of pyrophosphate concentration up to 500 μM (300 μM ATP has 200 μM PP_i ; 100 μM ATP has 400 μM PP_i , etc). This simulates ATP metabolism by cyclase (ATP is metabolized by cyclase into AMP and PP_i). (B) The same reaction conditions in (a), but treated with pyrophosphatase in the reaction (see Methods). Data is representative

SUPPLEMENTARY FIGURE 3

Correlation between activity and domain complementation in adenylyl cyclase demonstrated with a novel FRET sensor

Ritt, Sivaramakrishnan

Molecular Pharmacology



Supplementary Fig. 3. FRET readout of competitive inhibition of SYNAC by 1-deoxyforskolin.

FRET readout of SYNAC stimulated with 10 μM FSK in the presence of increasing concentrations of 1-deoxyforskolin. Red line is basal SYNAC activity and black line is 10 μM FSK stimulated SYNAC. The 300 μM deoxyforskolin point is significantly different from both basal and stimulated (Student's t-test, * = $p < 0.05$). Dashed lines indicate error bars (\pm SEM) for their respective colored lines. Data is mean \pm SEM of three independent repeats